ISSN 0021-3640, JETP Letters, 2024, Vol. 120, No. 8, pp. 547–553. © The Author(s), 2024. This article is an open access publication.
Russian Text © The Author(s), 2024, published in Pis'ma v Zhurnal Eksperimental'noi i Teoreticheskoi Fiziki, 2024, Vol. 120, No. 8, pp. 571–577.

FIELDS, PARTICLES, AND NUCLEI

Universal Momentum Distributions and Short-Range Nucleon Correlations

O. A. Rubtsova[a],* and V. N. Pomerantsev[a],**

[a] *Skobeltsyn Institute of Nuclear Physics, Moscow State University, Moscow, 119991 Russia*

**e-mail: rubtsova@nucl-th.sinp.msu.ru*

***e-mail: pomeran@nucl-th.sinp.msu.ru*

Received August 23, 2024; revised September 5, 2024; accepted September 7, 2024

The problem of constructing universal two-nucleon momentum distributions for main *NN*-configurations $^1S_0$ and $^3S_1-^3D_1$ used to describe short-range nucleon correlations in nuclei has been studied. A new method for calculating such distributions has been proposed, and their properties have been studied. As illustrations, calculations for several modern realistic *NN* potentials, including non-nucleon degrees of freedom, have been provided. A new characteristic that determines the ratio of the fractions of high-momentum components for spin-singlet and spin-triplet *NN* distributions at low energies, which can be useful for comparative evaluation of the isospin dependence of short-range correlations in calculations with different *NN* interaction potentials, has been proposed.

DOI: 10.1134/S0021364024602720

1. INTRODUCTION

In recent years, the problem of short-range correlations (SRC) in nuclei [1, 2] has become very relevant due to exclusive experiments on the electrodisintegration of nuclei $(e,e'NN)$ in quasi-elastic kinematics with the registration of three particles in coincidence [3]. Data on inclusive and semi-exclusive reactions are also continuing to be refined [4, 5]. The SRC problem is also studied in $(p,2pN)$ experiments curried out at the NICA facility [6, 7].

Comparison of experimental data with theoretical predictions based on the exact solution of the many-body problem with different nucleon–nucleon (*NN*) interactions would allow solving the SRC problem. However, due to the complexity of solving the scattering problem involving A nucleons, approximations are inevitably used to analyze SRC in nuclei with $A > 3$. The simplest of them is the plane-wave impulse approximation (PWIA), in which the quasi-elastic knock-out cross section $(e,e'NN)$ is proportional to the spectral function of nucleons in a nucleus or, with further simplification, to the corresponding two-nucleon momentum distribution ρ_{NN}. Up to this approximation, new exclusive experiments make it possible to reconstruct the momentum distributions of nucleons and to study the isospin dependence of SRC.

Two-nucleon momentum distribution ρ_{NN} in the nucleus depends on the relative momentum of nucleons $\mathbf{k}$, the momentum of their center of mass $\mathbf{Q}$, and the θ angle between them. An important property of these distributions is their factorization at high relative momenta k and low momenta of the center of mass Q, as well as scaling for two-nucleon (*nn*, *pp*, and *np*) momentum distributions in the region of high relative momenta. In a series of works by the research team headed by C. Ciofi degli Atti (see, for example, [8]), based on microscopic calculations for systems of A nucleons, it was shown that the momentum distributions for a number of light nuclei (^{3}H, ^{3}He, ^{4}He, ^{12}C, ^{16}O, and ^{40}Ca) at $Q < 1$–1.5 fm^{-1} and $k > 1.5$–2 fm^{-1} do not depend on the angle θ and are factorized as follows:

$$\rho^A_{NN}(\mathbf{k},\mathbf{Q}) = \rho^A_{NN}(k,Q,\theta) \approx C_A \rho_{NN}(k)\rho^A_{\mathrm{CM}}(Q), \quad (1)$$

where C_A is a constant depending on the nucleus A (the so-called nuclear contact), $\rho^A_{\mathrm{CM}}(Q)$ is the center-of-mass momentum distribution of a pair of nucleons, and $\rho_{NN}(k)$ is the function independent of the nucleus, i.e., a universal *NN* distribution. In the case of triplet *np* pairs, this universal distribution coincides with the distribution of nucleons in the deuteron: $\rho_{np}(k) = \rho_d(k)$.

Obviously, the factorization property of the two-nucleon momentum distribution assumes the existence of a similar universal distribution for spin-singlet pairs, i.e., *pp* and *nn* pairs, as well as spin-singlet *np* pairs. Since a pair of nucleons does not form a bound singlet state, the problem of obtaining such a universal distribution for a singlet pair arises. One of the possi-

ble solutions is to use the wavefunction of a virtual singlet state, an approximation of which can be constructed in the case of a separable NN interaction of nucleons [9]. Another option proposed within the generalized contact formalism [10, 11] is to use the scattering functions at zero energy that are normalized by the integral over the high-momentum part, both in the singlet and triplet channels. In this formalism, the nuclear momentum distributions (1) integrated over the momentum of the center of mass of the pair Q are used, which also turn out to be proportional in the high-momentum part to the constructed two-particle universal distributions for both the triplet and singlet channels. Note that the generalized contact formalism is widely employed at present to calculate various characteristics of SRCs in nuclei, as well as to parameterize electrodisintegration cross sections [12].

The aim of this work is to study in detail the properties of relative momentum distributions in bound and unbound pairs of nucleons interacting in vacuum, as well as to develop an alternative method for their calculation. According to the generalized contact formalism [10, 11], such distributions in the high-momentum region are be called universal momentum distributions (UMDs). Below, we will show that there is no need to solve the scattering problem strictly at zero energy to construct these distributions, and one can consider scattering wavefunctions at low energies, which expands the range of methods that can be used to calculate these distributions. Besides, we consider the effect of the nuclear medium on momentum distributions in infinite nuclear matter. In this paper, we also introduce a quantity that allows a quantitative comparison of the contributions from the high-momentum parts of the functions in the discrete and continuous spectra, which will be useful for estimating the relations between the pp and np correlations in nuclei for various NN interactions. Universal functions are calculated using the wave-packet continuum discretization method [13, 14], which is suitable for calculating scattering wavefunctions in free space and in nuclear matter.

2. METHOD FOR CONSTRUCTING UNIVERSAL MOMENTUM DISTRIBUTIONS

We consider the Lippmann–Schwinger equation for the wavefunction of a two-nucleon system with the definite values of spin σ in the momentum representation (we use units, where $\hbar = 1$):

$$\psi_{\mathbf{p}}^{(+)\sigma}(\mathbf{k}) = \psi_{\mathbf{p}}^{0\sigma}(\mathbf{k}) + \int d\mathbf{k}' \frac{V^{\sigma}(\mathbf{k},\mathbf{k}')\psi_{\mathbf{p}}^{(+)\sigma}(\mathbf{k}')}{\frac{p^2}{m} + i0 - \frac{k^2}{m}}, \qquad (2)$$

where ψ^0 is the free motion function (plane wave), V^{σ} is the NN potential, m is the nucleon mass, and $p = \sqrt{mE}$ is the relative on-shell momentum corresponding to the energy E. Below, for convenience, we will use the superscripts s and t to denote functions for the singlet ${}^1S_0$ and coupled triplet channels ${}^3S_1 - {}^3D_1$, respectively, and omit the superscript (+) in the wavefunction.

After the partial wave expansion, we obtain equations for the partial components of the wavefunction. Such an equation for the ${}^1S_0$ ($l = 0$ and $\sigma = 0$) channel has the form

$$\psi_p^s(k) = \frac{\delta(k-p)}{k^2} + \int_0^{\infty} \frac{dk'(k')^2}{2\pi^2} \frac{V^s(k,k')\psi_p^s(k')}{\frac{p^2}{m} + i0 - \frac{k^2}{m}}. \qquad (3)$$

These functions are normalized as $\int_0^{\infty} dk k^2 \psi_p^{*s}(k)\psi_{p'}^s(k) = \frac{\delta(p-p')}{p^2}$ and have a dimension different from the dimension of the discrete spectrum functions.

We define the high-momentum part of the integral of the square of the modulus of such a wavefunction as follows:

$$a_2^s(p) = \int_{p_0}^{\infty} dk k^2 |\psi_p^s(k)|^2, \qquad (4)$$

where p_0 defines the boundary of the high-momentum region. Note that $a_2^s(p)$ is a dimensional quantity and has the dimension of fm^3.

In the generalized contact formalism [11], the UMD for nn- and pp pairs is defined through the square of the modulus of the wavefunction obtained from the solution of equation (3) at $p = 0$ and normalized to unity in the high-momentum region. We consider such distributions for nonzero p as well. They can be obtained from the scattering wavefunctions by renormalization:

$$\rho_p^s(k) \equiv \frac{|\psi_p^s(k)|^2}{a_2^s(p)}. \qquad (5)$$

Note that since the momentum distribution is defined as the square of the modulus of the wavefunction, it does not matter which boundary condition the wavefunction satisfies.

It is convenient to use the wave-packet continuum discretization method [13] to calculate the wavefunctions. This method consists in dividing the momentum space (in each partial wave) into non-intersecting intervals of $\{\vartheta_i = [k_{i-1}, k_i]\}_{i=1}^N$ and introducing basis functions (free wave packets), the radial parts of which have the form:

$$x_i(k) = \frac{\theta(k \in \vartheta_i)}{k\sqrt{d_i}}, \quad d_i = k_i - k_{i-1}, \quad i = 1, \ldots, N, \qquad (6)$$

where the θ-function is non-zero and equal to unity if k belongs to the ϑ_i interval.

In the wave-packet basis, the wavefunction is represented as an expansion of $\psi_p^s(k) \approx \sum_{i=1}^{N} C_i x_i(k)$, and equation (3) is reduced to a system of algebraic equations:

$$\sum_{i'=1}^{N}(\delta_{ii'} - g_{0i}(p)V_{ii'})C_{i'} = \delta_{ii_0}, \quad i = 1,\ldots,N, \qquad (7)$$

where $g_{0i}(p)$ are the diagonal matrix elements of the resolvent of the free Hamiltonian, $V_{ii'}$ are the matrix elements of the interaction potential while the index i_0 determines the on-shell interval to which p belongs (see details in [13]). Thus, when projecting into the wave-packet basis, the delta function included in the inhomogeneous term of equation (3) is averaged so that equation (7) in the wave-packet basis does not contain singularities.

3. EXAMPLES OF MOMENTUM *NN*-DISTRIBUTIONS FOR DIFFERENT INTERACTIONS AND THEIR PROPERTIES

We consider momentum *NN* distributions (5), which are obtained from the solution of equation (7) at low energies. In this paper, we will use the value of $p_0 = 1.4$ fm^{-1} as the boundary of the high-momentum region.

Such distributions for channel $^1S_0$ found for the Nijmegen *NN* potential (type II) [15] are shown in Fig. 1. As can be seen in this figure, all distributions differ only at low momenta, and the functions have characteristic spikes near the on-shell momentum p corresponding to the averaged delta function included in the solution. However, in the high-momentum part, at $k > p_0$, all distributions coincide.

This property of wavefunctions becomes obvious if we consider the Schrödinger equation in the momentum representation:

$$\frac{k^2 - p^2}{m}\psi_p^s(k) + \int_0^\infty \frac{dk'(k')^2}{2\pi^2}V^s(k,k')\psi_p^s(k') = 0. \qquad (8)$$

It is easy to see that the solution of this equation in the region of $k \gg p$ is practically independent of p. Therefore, under the condition of normalization "to the tail" according to (5), all functions with $p \ll p_0$ actually coincide with each other in the high-momentum region of $k > p_0$. This property can be written as follows:

$$|\psi_p^s(k)|^2 \approx a_2^s(p)\rho^s(k), \quad k \geq p_0, \quad p \ll p_0, \qquad (9)$$

where the high-momentum part of the $\rho^s(k)$ distribution is independent of the on-shell momentum p.

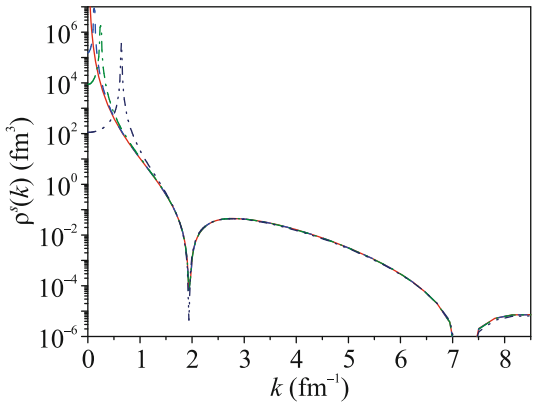

Fig. 1. (Color online) Momentum distributions in the $^1S_0$ channel constructed from continuum wavefunctions obtained with the Nijmegen potential at energies of (solid line) 0.0004, (dashed line) 0.62, (dash-dotted line) 2.5, and (dash-dot-dotted line) 17.15 MeV.

According to the factorization property, two-nucleon momentum distributions in nuclei at high momenta k are proportional to $\rho^s(k)$ [10].

Thus, to construct high-momentum parts of universal momentum *pp* distributions, there is no need to solve the Lippmann–Schwinger equation (or the Schrödinger equation) strictly at zero energy; it is sufficient to satisfy the condition of $p \ll p_0$.

We calculate the UMD for four types of potentials: Nijmegen (Nijm II) [15], CD Bonn [16], and two versions of the dibaryon model: Dib I [17] and Dib II [18]. The dibaryon model assumes the possibility of formation of an intermediate six-quark state (dibaryon) when nucleons approach each other. This leads to an effective *NN* interaction dependent on energy. Nevertheless, the wavefunctions for this model can be found by the same scheme as for energy-independent potentials. Both variants of the model considered here make it possible to reproduce the scattering amplitudes for the two main *NN*-configurations, but the corresponding wavefunctions differ in the region of high momenta.

Figure 2 shows the momentum distributions for *NN*-channel $^1S_0$ obtained in the wave-packet basis for the four considered potentials. As can be seen in this figure, the differences in the distributions under consideration are mainly determined by the positions of the minima (i.e., the zeros of the wavefunctions). The first minimum will determine the region of the minimum of *pp* correlations in nuclei, i.e., the region of the observed dominance of *np* correlations over *pp* correlations. For a "softer" CD Bonn potential, this minimum is shifted to the right while for the dibaryon model I, it is noticeably shifted to the left, to the region of lower momenta.

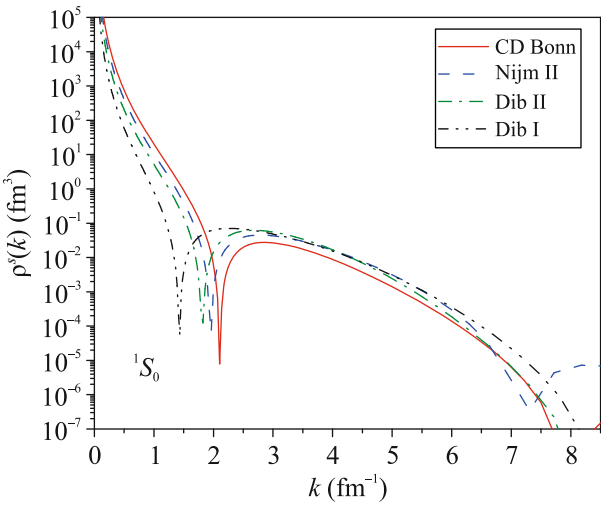

Fig. 2. (Color online) Momentum distributions in the $^1S_0$ channel evaluated with different NN potentials indicated in the legend.

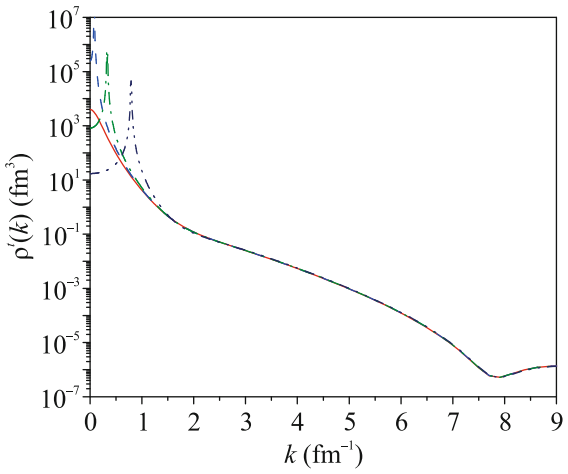

Fig. 3. (Color online) Momentum distributions in the $^3S_1$–$^3D_1$ channels constructed from functions obtained with the Nijmegen potential at energies of (solid line) –2.22, (dashed line) 0.275, (dash-dotted line) 4.52, and (dash-dot-dotted line) 25.96 MeV.

4. MOMENTUM DISTRIBUTIONS FOR THE SPIN-TRIPLET CHANNEL $^3S_1$–$^3D_1$

It should be noted that the momentum np distributions for the coupled channels $^3S_1$–$^3D_1$ have a similar property: the coincidence of high-momentum parts for the wavefunctions having the same normalization. Here, however, there is a bound state function, for which the momentum distribution is calculated through the square of the modulus of the momentum dependence of the deuteron wavefunction, $|\phi_d(k)|^2 \equiv |\phi_d^S(k)|^2 + |\phi_d^D(k)|^2$, as follows:

$$\rho^t(k) \equiv |\phi_d(k)|^2/a_2^d, \quad a_2^d = \int_{p_0}^{\infty} dk k^2 |\phi_d(k)|^2, \qquad (10)$$

where a_2^d is a dimensionless quantity that determines the contribution of high-momentum components to the momentum distribution for the deuteron [19].

We also construct the UMD from the scattering wavefunctions similarly to (5) with the inclusion of the S- and D-wave components of the wavefunction. In this case, the a_2 functions will be determined according to:

$$a_2^{t,l}(p) \equiv \int_{p_0}^{\infty} dk k^2 |\psi_p^{t,l}(k)|^2, \quad l = 0, 2, \qquad (11)$$

where the square of the modulus of the continuum wave function consists of the sum of the S- and D-components while the index l defines the channel with the incident wave.[1]

[1] Recall that at each p, there are two linearly independent solutions here.

The corresponding functions for the Nijmegen potential are shown in Fig. 3 in comparison with the momentum distribution for the deuteron that is normalized according to (10). Since all functions are the same in the high-momentum part, it is convenient to use the deuteron one as the universal np distribution.

Figure 4 shows the UMDs for triplet np pairs, i.e., for the coupled channels $^3S_1$–$^3D_1$, which are obtained from the deuteron momentum distribution $|\phi_d(k)|^2$ for various NN potentials with the normalization condition (10).

It should be noted that in [20, 21], the proportionality of the scattering wave functions at small distances

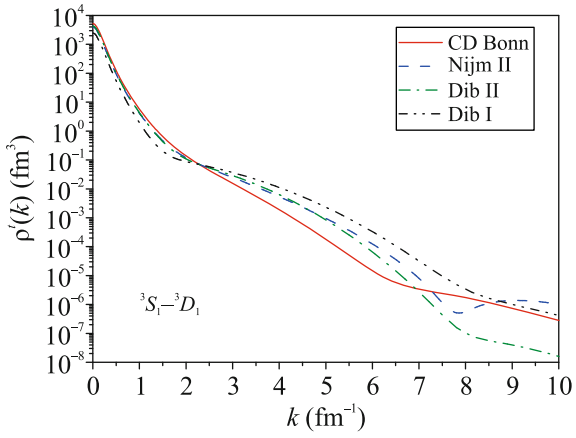

Fig. 4. (Color online) Momentum distributions in the $^3S_1$–$^3D_1$ channels evaluated with different NN potentials indicated in the legend.

(at low energies) and the bound state function in the coordinate space for the triplet S-wave interaction was proven based on the analytical continuation of the scattering wavefunctions to the deuteron pole. In essence, this is the same property that we demonstrated in this study for the high-momentum parts of the momentum distributions for the triplet channel, including the S- and D-wave components for realistic NN interaction potentials.

5. COMPARATIVE ESTIMATES OF HIGH-MOMENTUM CONTRIBUTIONS

The a_2^d quantity determines the fraction of the high-momentum part in the total momentum distribution of the deuteron. The values of this quantity differ significantly for different NN interaction models [19]. They are: 0.032 for the CD Bonn potential, 0.041 for the Nijmegen potential, 0.039 for the dibaryon potential II, and 0.068 for the dibaryon potential I.

The question arises of how to estimate the fractions of the high-momentum components for the scattering wave functions and, in particular, for the singlet channel. As was noted above, the quantities $a_2(p)$ that we introduced for the scattering wavefunctions are dimensional and cannot be compared directly with the a_2^d quantities for the bound state. However, it is possible to consider the total (integral) contribution from high-momentum components in each channel from the states with the on-shell momentum less than or equal to some q value ($q \ll p_0$), through the integrals:

$$A_2^s(q) = \int_0^q dpp^2 a_2^s(p), \quad A_2^t(q) = \sum_{l=0,2} \int_0^q dpp^2 a_2^{t,l}(p). \quad (12)$$

The ratio of these integral quantities in different channels (with the inclusion of the contribution from the bound state):

$$\eta(q) \equiv A_2^s(q)/(a_2^d + A_2^t(q)), \quad (13)$$

makes it possible to estimate the ratio of high-momentum components of the wavefunctions for the singlet and triplet channels at low energies for the considered NN interaction potential.

The ratio $\eta(q)$ is given in Fig. 5 for four considered NN interaction models. As can be seen in the figure, this ratio between the fractions of high-momentum components for the singlet and triplet channels turns out to be different for different potentials, i.e., is model-dependent. In this case, the contributions from the high-momentum components for the singlet channel at low energies are significantly smaller than those for the triplet channel ($\eta(q) \ll 1$) for all considered interactions. It is also clear that for the dibaryon model potentials, the relative high-momentum components for the singlet channel functions are larger than those for the traditional meson-exchange potentials. In this case, although the universal functions for the dibaryon potential II and for the Nijmegen potential for the singlet and triplet channels are very close to each other (see Figs. 2 and 4) up to momenta about 7 fm^{-1}, the ratio $\eta(q)$ for the dibaryon potential turns out to be noticeably larger, which will most likely lead to stronger pp correlations in nuclei.

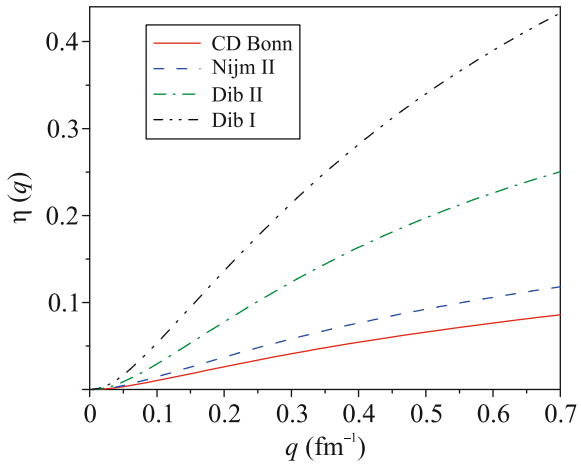

Fig. 5. (Color online) Ratios $\eta(q)$ for the singlet and triplet channels obtained with different NN potentials indicated in the legend.

Thus, the proposed $\eta(q)$ value complements the a_2^d parameter used in the literature for the bound state and allows a preliminary comparative estimate of the isospin dependence of the SRC for different NN interaction potentials.

6. MOMENTUM DISTRIBUTIONS OF NUCLEONS IN A NUCLEAR MEDIUM

As another illustration, we consider the high-momentum behavior of momentum distributions in nuclear medium. It was shown earlier [14] that it is possible to determine the effective Hamiltonian for a pair of nucleons above the Fermi surface. In a certain range of densities, this Hamiltonian has bound states (states with energies below the double Fermi energy $2e_F$), both for the triplet and singlet channels.[2]

Next, we study the high-momentum components of the wavefunctions of such bound states. In the momentum representation, the wavefunction of such a state in the $^1S_0$ channel at zero momentum of the center of mass satisfies the equation:

$$\frac{k^2 - k_B^2}{m}\psi_B^s(k) + \int_{k_F}^{\infty} \frac{dk' k'^2}{2\pi^2} V^s(k,k')\psi_B^s(k') = 0, \quad (14)$$

[2] Such states correspond to the eigenfunctions of the kernel of the Bethe–Goldstone equation with unit eigenvalues.

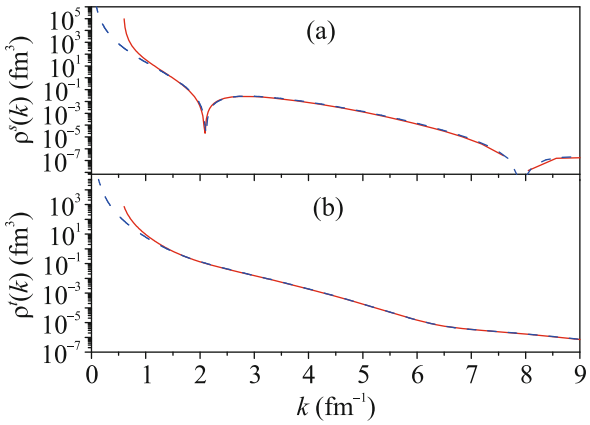

Fig. 6. (Color online) (Solid lines) Momentum distributions in the (a) $^1S_0$ and (b) $^3S_1$–$^3D_1$ channels that were found in calculations in a nuclear medium based on Eq. (14) with the CD Bonn potential in comparison with (dashed lines) the universal momentum distribution for the same potential.

where k_F is the Fermi momentum for the considered medium while the equation is solved in a subspace of $k, k' \geq k_F$ (the so-called Pauli-allowed subspace). In this case, the energy of the bound state is negative and is determined from the relation: $E_B = \frac{k_B^2}{m} - 2e_F$, where $e_F = \frac{k_F^2}{2m}$.

A method for calculating such states in the same wave-packet basis that we used above is described in [14]. These functions are normalized to unity, so dimensionless factors $a_2^{s,t}$ can be introduced to normalize them to the high-momentum part. Figure 6 shows the momentum distributions for the bound states of two nucleons in the nuclear medium in the singlet and triplet channels at the Fermi momentum of $k_F = 0.6$ fm^{-1} for the CD Bonn potential in comparison with the UMD for the same interaction obtained above. In the high-momentum parts, the compared functions are practically indistinguishable, which confirms the universality of two-nucleon SRCs. The obtained fractions of the high-momentum components for the singlet and triplet functions are $a_2^s = 0.0018$ and $a_2^t = 0.041$, respectively. Despite the fact that the singlet nucleons are bound here, a significant excess of the contribution of the high-momentum component for the triplet channel is again observed compared to the singlet one. We also found the fractions of the high-momentum components for the other two interactions considered in this study. The a_2^s/a_2^t ratios at $k_F = 0.6$ fm^{-1} for different *NN* potentials are as follows: 0.044 (CD Bonn), 0.058 (Nijm II), and 0.142 (Dib II). As we can see, these ratios are arranged in the same sequence as the $\eta(q)$ curves shown in Fig. 5 for *NN* interactions in vacuum.

7. CONCLUSIONS

It has been shown that, under the selected condition of normalization to the high-momentum part, two-particle scattering wavefunctions can be used as universal momentum distributions at any sufficiently low energy. This property opens wide possibilities for calculating such distributions. In this study, the wave-packet continuum discretization method was used, but any other approaches that are traditionally used to calculate scattering wavefunctions can also be employed here. In particular, pseudo-states of the Hamiltonian obtained in the L^2 basis can be used to construct universal distributions if the basis allows describing the high-momentum region. We are planning this study in the future.

In the paper, we have also proposed the ratio $\eta(q)$ that allows comparing the contributions of the high-momentum components for the spin-singlet and spin-triplet channels at low energies. Such a function depends on the used *NN* interaction model and can serve as an additional characteristic of the isospin dependence of the SRC.

Besides, we have studied the momentum distributions corresponding to bound states of correlated pairs of nucleons above the Fermi surface in the nuclear medium. The momentum distributions for such states in the region of large momenta have been shown to be proportional to the universal *NN* distributions.

FUNDING

The work was supported by the Russian Science Foundation, project no. 23-22-00072, https://rscf.ru/project/23-22-00072/.

CONFLICT OF INTEREST

The authors of this work declare that they have no conflicts of interest.

REFERENCES

1. C. Ciofi degli Atti, Phys. Rep. **590**, 1 (2015).
2. J. Arrington, N. Fomin, and A. Schmidt, Ann. Rev. Nucl. Part. Sci. **72**, 307 (2022).
3. M. Duer, O. Hen, E. Piasetzky, et al. (CLAS Collab.), Nature (London, U.K.) **560**, 617 (2018).
4. S. Li, R. Cruz-Torres, N. Santiesteban, et al. (Collab.), Nature (London, U.K.) **609**, 41 (2022).
5. R. Cruz-Torres, D. Nguyen, F. Hauenstein, et al. (Jlab Hall A Tritium Collab.), Phys. Rev. Lett. **124**, 212501 (2020).
6. M. Patsyuk, J. Kahlbow, G. Laskaris, et al. (The BM@N Collab.), Nat. Phys. **17**, 693 (2021).
7. A. B. Larionov and Yu. N. Uzikov, Phys. Rev. C **109**, 064601 (2024).
8. M. Alvioli, C. Ciofi degli Atti, and H. Morita, Phys. Rev. C **94**, 044309 (2016).
9. Yu. N. Uzikov and A. Uvarov, Phys. Part. Nucl. **53**, 426 (2022).
10. R. Cruz-Torres, D. Londaroni, R. Weiss, M. Piarulli, N. Barnea, D. W. Higinbotham, E. Piasetzky, A. Schmidt, L. B. Weinstein, R. B. Wiringa, and O. Hen, Nat. Phys. **17**, 306 (2021).
11. R. Weiss, R. Cruz-Torres, N. Barnea, E. Piasetzky, and O. Hen, Phys. Lett. B **780**, 211 (2018).
12. R. Weiss, A. W. Denniston, J. R. Pybus, O. Hen, E. Piasetzky, A. Schmidt, L. B. Weinstein, and N. Barnea, Phys. Rev. C **103**, L031301 (2021).
13. O. A. Rubtsova, V. I. Kukulin, and V. N. Pomerantsev, Ann. Phys. (Amsterdam, Neth.) **360**, 613 (2015).
14. H. Müther, O. A. Rubtsova, V. I. Kukulin, and V. N. Pomerantsev, Phys. Rev. C **94**, 024328 (2016).
15. V. G. J. Stoks, R. A. M. Klomp, C. P. F. Terheggen, and J. J. de Swart, Phys. Rev. C **49**, 2950 (1994).
16. R. Machleidt, Phys. Rev. C **63**, 024001 (2001).
17. V. I. Kukulin, I. T. Obukhovsky, V. N. Pomerantsev, and A. Faessler, Int. J. Mod. Phys. E **11**, 1 (2002).
18. V. I. Kukulin, V. N. Pomerantsev, O. A. Rubtsova, M. N. Platonova, and I. T. Obukhovsky, Chin. Phys. C **46**, 114106 (2022).
19. F. Sammarruca, Phys. Rev. C **92**, 044003 (2015).
20. G. Fäldt and C. Wilkin, Phys. Lett. B **382**, 209 (1996).
21. G. Fäldt and C. Wilkin, Am. J. Phys. **66**, 876 (1998).

Translated by A. Ivanov